Ultra-thin single crystal silicon modules capable of 450 W/kg and bending radii <1mm: fabrication and characterization

Jose L. Cruz-Campa, Gregory N. Nielson, Murat Okandan, Paul J. Resnick, Carlos A. Sanchez, Janet Nguyen, Benjamin B. Yang, Alice C. Kilgo, Christine Ford, Jeff S. Nelson

Sandia National Laboratories, Albuquerque, NM, M.S. 1069, 87123, USA.

***Abstract* — We present ultra-thin single crystal mini-modules built with specific power of 450 W/kg capable of voltages of >1000 V/cm^2. These modules are also ultra-flexible with tight bending radii down to 1 mm. The module is composed of hundreds of back contact microcells with thicknesses of approximately 20 µm and diameters between 500-720 µm. The cells are interconnected to a flexible circuit through solder contacts. We studied the characteristics of several mini-modules through optical inspection, evaluation of quantum efficiency, measurement of current-voltage curves, and temperature dependence. Major efficiency losses are caused by missing cells or non-interconnected cells. Secondarily, damage incurred during separation of 500 µm cells from the substrate caused material detachment. The detachment induced higher recombination and low performance. Modules made with the larger cells (720 µm) performed better due to having no missing cells, no material detachment and optimized AR coatings. The conversion efficiency of the best mini module was 13.75% with a total V_{oc} = 7.9 V.**

***Index Terms* — photovoltaic cells, solar energy, silicon, thin film devices, flexible electronics.**

I. Introduction

Photovoltaics (PV) have the potential to be the power source of choice for a wide variety of products. Flexible PV extends the potential application of solar power generation to portable electronics and transportation. For solar to be embedded in such applications, the weight, specific power, flexibility, moldability, voltage, and appearance of the technology all become important factors.

Light weight and high specific power solar cells have been a target for space applications. Early trials for achieving high specific power have improved from 45 W/kg in the year 2000 to 180 W/kg in 2004 [1] using Fresnel concentrators made of curved, flexible silicone and III-V cells. Recently, values of up to 3.2kW/kg under AM 1.5G spectra were demonstrated in prototypes using thin film approaches with efficiencies up to 9.5%; however, no data on the material stability were presented [2]. The private sector has realized the potential of high specific power and has demonstrated values around 1kW/kg with III-V materials and epitaxial lift off [3]. The disadvantage of using large sheets of III-V is the fragility and cost of these devices. These efforts prove the feasibility of achieving high specific power modules. In most cases flexible, low price and high efficiency modules are desirable. Traditional crystalline materials such as silicon and III-V have shown the highest efficiency but are built on rigid substrates. Among flexible/moldable solar cells, most organic PV and some thin film technologies have proved capable of high flexibility with the trade-off of significantly lower efficiencies.

In this paper we describe a technology that has high specific power at relatively high efficiencies and potentially low cost using thin crystalline silicon, a reliable and well understood semiconductor. Thin crystalline silicon cells can have higher open-circuit voltage, increased fill factor, and greater tolerance for radiation in outer space [4] compared to thicker silicon. Single crystal silicon was chosen due to its abundance, low cost, stability, performance characteristics, and compatibility with traditional processing tools. The silicon is about 10 times thinner (approximately 20 µm) compared to commercial silicon cells, making it very fragile in large formats such as wafers. To address this fragility we made very small diameter silicon cells to increase robustness. We call this "ultra-thin segmented silicon" [5] and we have demonstrated segments ranging in size from 250 µm to 1 mm in diameter. The segmentation aids with the flexibility when cells are combined to form modules and mitigates yield loss due to silicon breakage. In this article we only show the results for mini-modules using cells with diameters of 500 µm and 720 µm. Since each cell produces about 0.45 V at maximum power point, very high voltages are achievable in very small areas. Fig. 1 shows achievable voltages/cm^2 as a function of the diameter of the cell, measured from corner to corner of the hexagonal shaped cell. Voltages of 1000V/cm^2 are easily achieved with cells on the order of 250 µm.

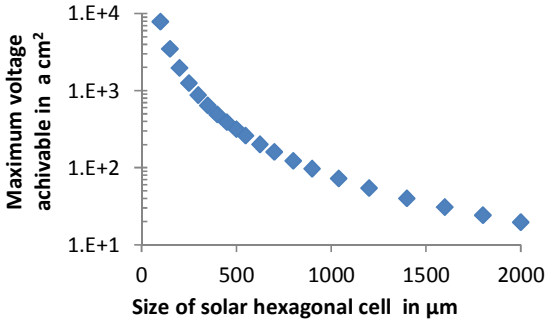

Fig. 1. Graph showing capability of micro cells to achieve high voltages in small areas by connecting them in series.

The large number of cells in a module allow for numerous series and parallel interconnection schemes. This enables the module designer to target a wide voltage/current range. Furthermore, multiple parallel connections enhance the reliability and shade tolerance of the product [6].

Ultra-thin formats enable seamless integration of solar powered charging capability into conventional electronic devices without increasing the weight or compromising product design considerations. We envision that this technology could be used in consumer electronics, toys, cars, planes and anywhere where there is light and a need to generate power. Fig. 2 shows a photograph of a bent mini-module containing hundreds of interconnected and functional micro cells.

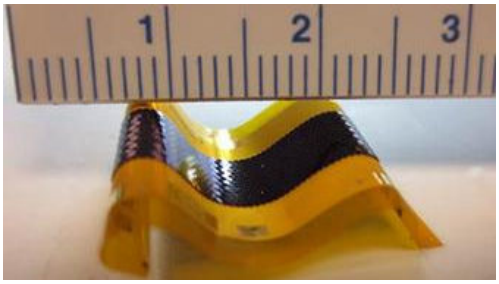

Fig. 2. Bent flexible solar mini-module. It can be seen that curvatures of about 1 mm can be obtained. The subdivisions of the ruler are in mm.

II. Fabrication

The cells are created in standard thickness, 150 mm wafers using CMOS/MEMS tools. This reduces the possibility of breakage and enhances yield. After the processing of the wafer is complete, thousands of fully-functional, ultra-thin microcells are weakly attached to the handle wafer. Then, a transfer onto flex circuits occurs to produce the final product of flexible, ultra-thin solar cells. The handle wafer can potentially be reused after the transfer thus bringing down material costs. Fig. 3 shows a) fully processed wafer with thousands of microcells prior to the transfer step onto flex circuits; b) flex circuit pattern that will receive the cells; c) mounted and interconnected cells on the flexible substrate.

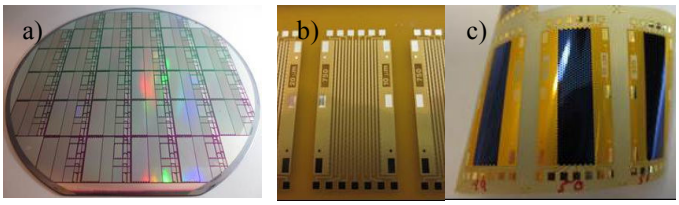

Fig. 3. a) Fully processed wafer b) flex circuit c) solar cells mounted on flex circuit

The fabricated cells have interdigitated back point contacts. Creating these cells require a series of implantations, etches, metal depositions, and film growths. The process is very similar to those used in fabricating microchips and MEMS (micro electrical mechanical systems). The details about these processes are presented elsewhere [7]-[8]. At the end of the fabrication, the cell is fully functional and attached to the handle substrate by thin tethers or anchors as shown in Fig. 4 and Fig. 5. The cells' electrical contacts are formed by interdigitated metal traces on the surface that connect to the two main electrode pads. The positive pad and its fingers connect to all of the p-type implantations through an insulating silicon nitride layer. The negative pad connects in the same way to all of the n-type implantations.

After metal bond pads have been lithographically defined, tin-lead solder bumps are electrodeposited to allow mounting of the cells onto the flexible circuit. Fig. 4 shows the back of the cells in detail. The front of the cells (not shown) has zero metal shading.

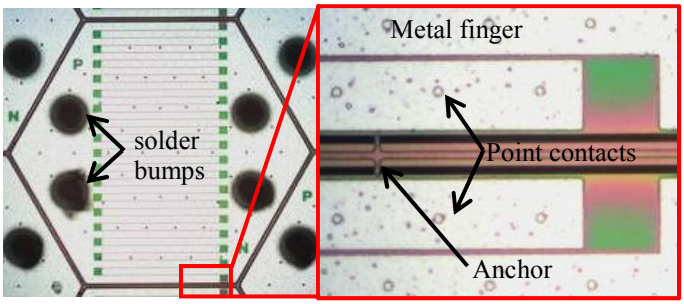

Fig. 4. The left picture shows the back of one solar cell. The diameter of the cell from corner to corner of the hexagon is 720 µm. The right picture zooms into a section of the cell to show the interdigitated fingers, point contacts, and anchors.

The solder bumps serve a dual purpose: 1) they enable the mechanical transfer of the cells to the flexible platform and, 2) they become the electrical contacts between the cell and the flexible interconnecting circuit board. The assembly requires good alignment between the cells and the flex circuit, which is done using standard tools common in the microelectronics industry. After the flex circuit and the cells are aligned and in physical contact with each other, the entire stack made up of the cells along with the flex circuit is heated up to the melting temperature of the solder (around 230°C).

Once the solder wets the receiving substrate, the temperature is lowered so the solder can harden. After the stack is cooled below the melting temperature of the solder, the cells are electrically and mechanically connected to the flexible circuit. At this point the flex circuit is physically pulled and all the anchors attaching the cells to the handle wafer are broken, thus completing the transfer of the cells to the flex circuit. Fig. 5 is a cross section diagram explaining

the main components of the system and the module assembly process.

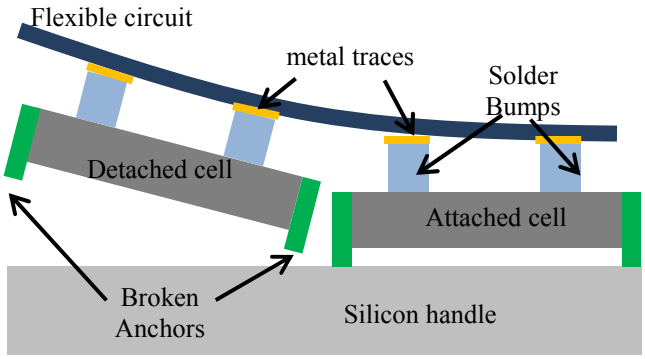

Fig. 5. Simplified cross section explaining transfer of the cells from wafer to flex circuit.

Following the transfer of the cells, a final etch is done to remove residual layers on the front of the cell and to adjust the thickness of the AR coating. Fig. 6 shows a polished cross section of a finished mini-module showing the aspect ratios and the components of a single cell.

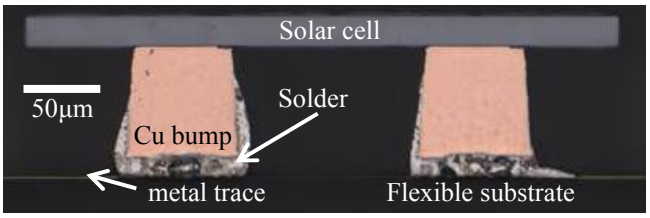

Fig. 6. Polished cross section of solar cell connected to the flexible receiving substrate

Post-fabrication, the mini-modules were bent and flexed to verify that all of the cells were firmly attached. Afterwards, the mini-modules were tested under light to verify that they are functional. Fig. 7 shows a photograph of a mini-module being electrically tested as it was being flexed. The module output V_{oc} stays above 7 Volts for all possible flexures.

Fig. 7. Voltage measurement of the mini-module while being flexed.

III. Characterization and Results

A total of 15 mini-modules were completed for this study. Three of these modules had larger cells (720 µm in diameter) and 12 had smaller cells (500 µm in diameter). In the modules containing 720 µm-diameter cells, 14 sets of 34 cells in parallel were wired in series for a total of 476 cells. For the 500 µm cell modules, 14 sets of 47 cells in parallel were wired in series for a total of 658 cells. Efficiencies ranged from 4.9% to 13.7% with an average of 8% and a standard deviation of 2.9%.

All of the modules were analyzed to understand the differences that made some modules better than others. In this paper we present the results from the most and the least efficient modules for simplification. A visual inspection using optical microscopy revealed obvious differences in the cells. Fig. 8 (left) shows the mini-module with highest efficiency and Fig. 8 (right) the mini-module with the lowest efficiency. Through the inspection it was seen that in some cases cells were missing. Also, by studying the spaces formed by missing cells, we found that incorrect alignment led to poor adhesion and bad contact. An incomplete suspension of cells was also observed as evidenced by pieces of silicon being torn off of the cells during the transfer step. Finally, the average thickness of the AR coating in the most efficient module was about 64nm and the thickness on the least efficient module was about 85nm. All of these factors resulted in a less efficient cell. The best performing mini-module did not have missing cells, misalignments, or tear offs. From analyzing the 15 mini-modules, we determined that misalignment and missing cells had the largest impact in efficiency, followed by high recombination due to torn off silicon. AR coating played a minimum role but influenced the current to a small degree.

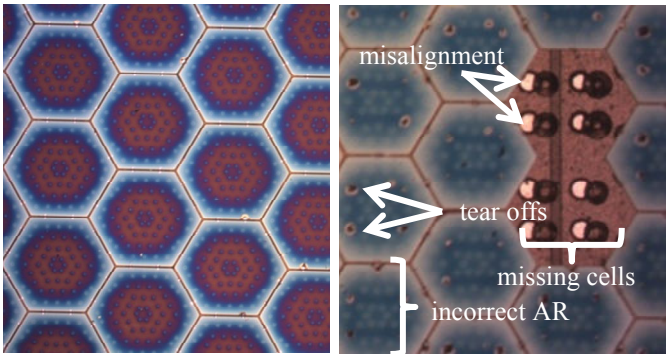

Fig. 8. Left. - Section of the highest efficiency module (720 µm cells). Right. - Module showing all problems presented in the process (500 µm cells).

The presence of torn off silicon (the main efficiency impacting factor after missing cells) and the incorrect thickness of the AR coating (secondary factor) led to a poor external quantum efficiency (EQE). This can be seen in Fig. 9. The quantum efficiency measurement (related to the

absorption in the cell) was done using a Newport Oriel ® IQE-200. It can be seen from Fig. 9 that the absorption in the 4% efficiency module is lower for all wavelengths, particularly at shorter wavelengths. This result suggests that the tear offs produced a higher surface recombination velocity thus trapping carriers with high energy. The non-optimal absorption at long wavelengths was observed for all modules regardless of efficiency. Since the cells are thin, not all light was absorbed. This can be observed on the tail to the right as the light approaches the band edge of silicon. In future iterations of cells, we are considering light trapping features to enhance the response in the infrared.

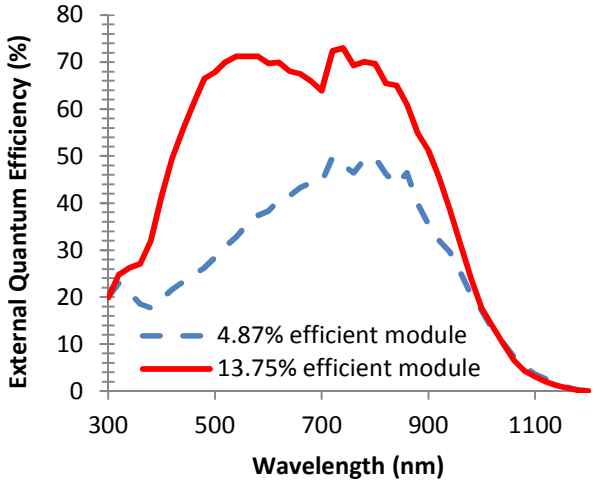

Fig. 9. External quantum efficiency of the most and least efficient mini-modules

In order to corroborate the observations of the EQE, a dark current density vs. voltage measurement of the modules was done (dark current-voltage or dark JV). From Fig. 10, it can be seen that the diode characteristics between the 4% and the 13% efficient cells differ. The 13% cell has a J_{oe} of 2.8 $X10^{-11}$ A/cm^2 and the one for the 4% 2.6 $X10^{-9}$ A/cm^2. The higher current density suggests that there is greater carrier recombination in the 4% module than in the 13% one. Passivation of the cell can be further improved given that other high-performing cells have achieved values as small as 2.5 $X10^{-14}$ A/cm^2 [9] for J_{oe}. By comparing mini modules that did not have missing cells but that did have missing silicon due to tear offs, we can attribute up to 2.5% absolute efficiency losses due to recombination.

Another effect observed in the dark current-voltage measurement was that the slope of the 4% efficient module's dark JV curve is smaller than the 13% module, and the current-voltage response is not as linear. This difference is due to the non-uniform current generated by the parallel circuits with missing cells, and has direct implications to the fill factor.

As confirmed by the EQE and dark JV curves, the absorption was diminished due to non-optimized AR coatings and a higher recombination velocity on the surface. The higher recombination velocity (related to J_{oe}) will also lower the voltage of the cell by a small amount. Fig. 11 shows the current voltage curve of the tested mini-modules under illumination (light JV). An OAI TriSOL 1800 nm class AAA solar simulator was used as the light input running in constant intensity mode. The solar spectrum was normalized to an intensity of 1000 W/m^2 (using a silicon reference cell). The cell was kept in contact with a temperature controlled stage at 25°C during the measurement. The JV curve was measured using an Agilent B1500 source-meter. The area of the module represents the region of the arrays of cells including the area associated with the gaps between cells. The metrics for both mini-modules are shown in Table 1.

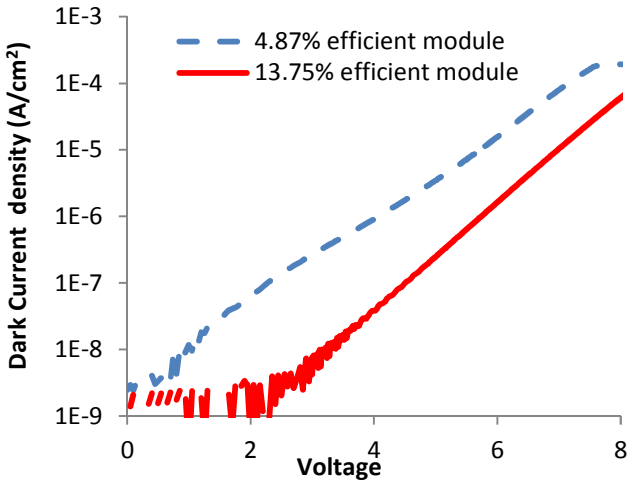

Fig. 10. Dark current density curve vs. voltage for the best and worst cell measured.

TABLE I
METRICS OF MODULES

Efficiency	4.8%	13.7%
Area	1.14 cm^2	1.59 cm^2
I_{sc}	1.6mA	3.69 mA
V_{oc}	5.87 V	7.9 V
P_{max}	5.57 mW	21.8 mW
V_{max}	4.3 V	6.4 V

Through comparison of minimodules with the same AR coating and no tear offs, we determined that missing cells had the biggest impact on efficiency. Up to 5% absolute losses in efficiency was attributed to having missing cells. Missing cells will lower the total current of the mini module and decrease the fill factor (the modules are formed by series combinations of strings of cells connected in parallel).

In order to calculate the specific power of the best module, we obtained the maximum power (21.85 mW) from the current voltage (IV) curve and divided it by the weight of the module (48mg grams) yielding a specific power or 455W/kg. Commercial foldable (not highly bendable) modules have specific powers between 20-40 W/kg [10]-[11].

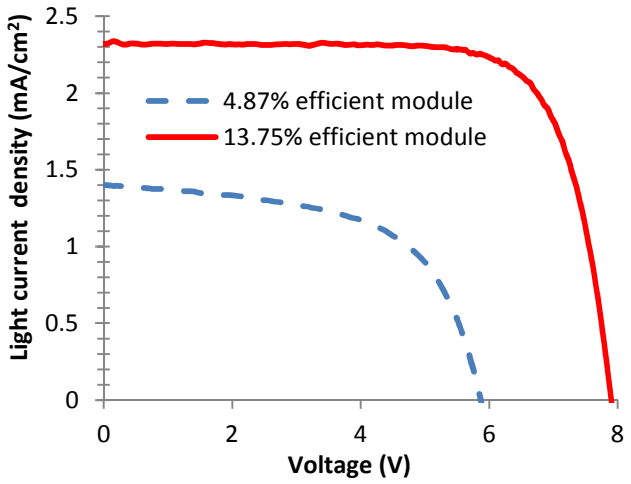

Fig. 11. JV curve of the best and worst module under 1 sun AM 1.5G illumination.

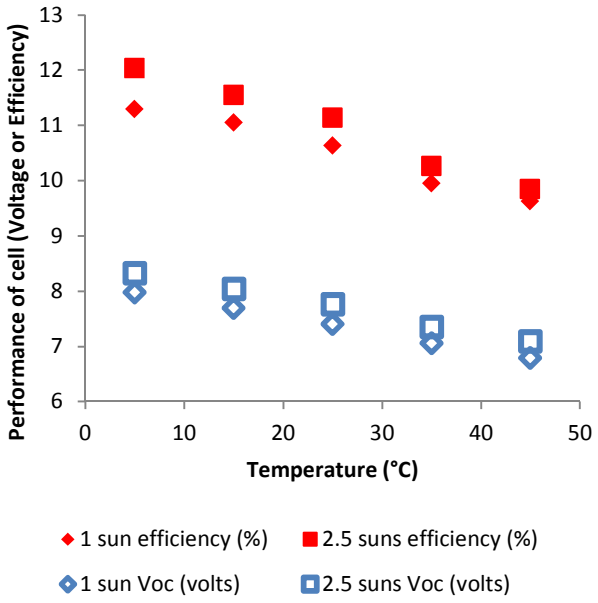

Fig. 12. Voc and efficiency of a 10.7% efficiency module vs. temperature at two different light intensities.

Finally, a temperature dependence study at two different light intensities was performed. This study was done to analyze the behavior of silicon in micro-sized cells. The temperature ranged from 5°C to 45 °C and the two intensities used were 1Sun and 2.5Suns. The temperature was varied using an INSTEC STC200 temperature controlled stage and the light intensity was varied using a Fresnel lens. JV curves of one module (nominal efficiency of 10.7% under normal conditions) were taken. The efficiency and open circuit voltage was extracted from the JV curves. Fig. 12 shows the efficiency (red) and open circuit voltage (blue) of the mini-module for two different light intensities: 2.5 suns (squares) and 1 sun (diamonds) vs. the temperature.

The cells exhibited the temperature and light intensity dependence expected for macroscopic silicon solar cells. Higher efficiencies and open circuit voltages were observed at both lower temperatures and higher intensities.

The slope of the Voc curve is 30mV/°C for the whole module or 2.14V/°C for each cell (there are 14 cells connected in series) which agrees with the known 2.1-2.3mV degradation per degree. This study revealed that micro sized solar silicon cells have the same behavior as traditional macroscopic cells.

IV. Path for Higher Efficiencies and Lower Weight

We have identified the critical steps that can improve the performance and increase the specific power of these devices. Enhanced passivation will lead to a higher V_{oc}. AR coating uniformity and optimized thickness will lead to higher currents, enhancing alignment of placing and reducing missing cells will improve overall efficiency. All of these steps will lead to higher efficiencies without adding significant weight and thus achieving higher specific power. Other areas of interest are the reduction of solder bump height and diameter, minimizing the thickness of the conductors in the flexible circuit, and finally reducing the thickness of the flex substrate and cover material, all of which will reduce the weight of these already very lightweight solar modules. In future iterations, implementing light trapping structures could further increase light collection. The combination of high efficiency with a lightweight interconnection board culminates in solar modules with increased specific power.

IV. Conclusions

We presented the fabrication and characterization of ultra-thin single crystal mini-modules with a current specific power of 450 W/kg that are capable of voltages >1000 V/cm^2. The modules consist of arrays of ultra-thin and small silicon cells interconnected through solder bumps and flexible substrates. They are bendable with very tight bending radii (1 mm). Studies of the characteristics of several mini-modules using EQE, dark and light JV, and optical inspection were shown for the worst and best mini-module. The main factor for low efficiencies was missing cells (up to 5% absolute losses of efficiency). The secondary factor was insufficient release of the cells, particularly in the 500 µm cells. This caused incomplete suspension, damaging the cell surface, causing higher recombination, and thus lowering performance of

those modules. Larger cells (720 μm) performed better due to no material detachment, fewer missing cells, and optimized AR coatings. The conversion efficiency of the best mini module was 13.75% with a total V_{oc} = 7.9 V and a specific power of 455W/kg.

ACKNOWLEDGEMENTS

Sandia National Laboratories is a multi-program laboratory managed and operated by Sandia Corporation, a wholly owned subsidiary of Lockheed Martin Corporation, for the U.S. Department of Energy's National Nuclear Security Administration under contract DE-AC04-94AL85000.

REFERENCES

[1] M. J. O'Neill, "1,000 W/kg Solar Concentrator Arrays for Far-Term Space Missions", *in AIP Conf. Proc. 699*, 2004, pp. 875-882.

[2] N. Wyrsch, D. Dominé, F. Freitas, L. Feitknecht1, Bailat, C. Ballif, G. Poe, K. Bates, K. Reed, "Ultra-Light Amorphous Silicon Cell For Space Applications", *in IEEE 4th World Conference on Photovoltaic Energy Conversion*, 2006, pp. 1785 - 1788.

[3] http://mldevices.com/products-a-services/photovoltaics

[4] G. A. Landis, "A process sequence for manufacture of ultra-thin light trapping silicon solar cells," *Solar Cells*, vol. 29, no. 2–3, pp. 257–266, 1990.

[5] J. L. Cruz-Campa, et al. "Ultra-thin Flexible Crystalline Silicon: Microsystems-Enabled Photovoltaics", *Journal of Photovoltaics* vol. 1, pp. 3-8, 2011.

[6] A. L. Lentine et al. "Optimal cell connections for improved shading, reliability, spectral performance of microsystem enabled photovoltaic (MEPV) modules", *in 35th IEEE PVSC*, 2010, pp. 3048-3054.

[7] G. N. Nielson et al. "Microscale C-SI (C) PV Cells For Low-Cost Power", *in 34th IEEE PVSC,* 2009, pp. 1816-1821.

[8] J. L. Cruz-Campa, et. al.; "Microsystem Enabled Photovoltaics: 14.9% efficient 14μm thick crystalline silicon solar cell" *Solar Energy Materials and Solar Cells,* vol. 95-2 pp. 551-558, 2011.

[9] J. Zhao, A. Wang, A. Aberle, S. R. Wenham, and M. A. Green, "717-mV open-circuit voltage silicon solar cells using hole-constrained surface passivation", Appl. Phys. Lett., Vol. 64-2 pp. 199-201, 1994.

[10] www.sacredsolar.com

[11] www.globalsolar.com/downloads/PowerFLEX_6m.pdf